NASA TECHNICAL NOTE

NASA TN D-5300

NASA TN D-5300

APPLICATIONS OF QUASILINEARIZATION THEORY TO SYSTEM IDENTIFICATION

by George A. Zupp, Jr., and S. Bart Childs

Manned Spacecraft Center
Houston, Texas

NATIONAL AERONAUTICS AND SPACE ADMINISTRATION • WASHINGTON, D. C. • JULY 1969

APPLICATIONS OF QUASILINEARIZATION THEORY TO SYSTEM IDENTIFICATION

By George A. Zupp, Jr., and S. Bart Childs

Manned Spacecraft Center
Houston, Texas

NATIONAL AERONAUTICS AND SPACE ADMINISTRATION

For sale by the Clearinghouse for Federal Scientific and Technical Information
Springfield, Virginia 22151 – CFSTI price $3.00

ABSTRACT

The theoretical development and application of quasilinearization techniques to problems of system identification are presented. A one-degree-of-freedom system is used for the examples for the identification problems. Several numerical experiments are presented that relate the effects of noisy input data to the accuracy obtained in computing unknown parameters of the governing differential equations. Also presented are the application of quasilinearization to the identification problems of automobile coasting and parachute dynamics. Conclusions from these experiments are included.

APPLICATIONS OF QUASILINEARIZATION THEORY TO SYSTEM IDENTIFICATION

By George A. Zupp, Jr., and S. Bart Childs*
Manned Spacecraft Center

SUMMARY

The theoretical development and application of several quasilinearization techniques to system-identification problems are described. Presented in the theoretical development of the quasilinearization techniques are (1) the definition of system identification, (2) the development of the Newton-Raphson method for solving nonlinear simultaneous algebraic equations, and (3) the extension of the Newton-Raphson method by Kantorovich to the solution of nonlinear or linear differential equations subjected to multipoint boundary conditions.

System-identification problems are solved for four one-degree-of-freedom systems, a linear and a nonlinear oscillator, a free-falling parachute, and a coasting automobile. Several numerical experiments are presented to relate the effects of noisy data to the accuracy with which the coefficients and initial conditions of the governing differential equations can be computed. Experimental data were available for the free-falling parachute and the coasting automobile. The aerodynamic drag-area parameter was determined in both instances by quasilinearization. Numerical examples are presented to relate the accuracy of the predicted aerodynamic drag-area parameters to inaccuracies in the experimental data for the free-falling parachute and coasting automobile.

INTRODUCTION

The analysis of a physical phenomenon usually starts with the postulation of an equivalent mathematical model, which is usually in the form of a differential equation (or equations). In differential-equation form, the coefficients and initial conditions usually have physical significance, and a knowledge of their values can lead to a better understanding of the physical phenomenon. Determination of the initial conditions and coefficients (unknown parameters) of the governing differential equations by "closed form" analytical methods is not always possible. In certain instances, measured observation of the phenomenon can be used in determining the unknown parameters. Determination of the unknown parameters of governing differential equations by using

*Associate Professor of Mechanical Engineering, University of Houston, Houston, Texas.

measured observations of the phenomenon is called system identification. This report presents the development and application of several quasilinearization techniques to the solution of system-identification problems. Consideration is given to the effect of "random" noise on the identification of nonlinear systems. Additive noise or bias errors in the data are not considered.

Standard system-identification techniques for dynamics problems commonly rely on sophisticated instrumentation to measure the state variables necessary to identify the system. The accuracy to which a state variable can be measured is dependent on the measuring technique; however, the higher the order of the state variable being measured, the noisier the measurements usually are. Any estimates of the unknown parameters, based on experimental data of the system-identification problem, reflect these experimental errors. Therefore, experimental data of highest accuracy should be used in the prediction of the unknown parameters of the system-identification problem.

Two quasilinearization techniques can be used to calculate the unknown parameters of the system-identification problems that contain experimental data. These quasilinearization techniques essentially determine the coefficients and initial conditions of the governing differential equations that "best" satisfy the experimental data. These techniques are (1) the Newton-Raphson method for solving sets of nonlinear algebraic equations, which are the solutions to the governing differential equations, and (2) the Newton-Raphson-Kantorovich method for solving system-identification problems for which closed-form solutions of the governing differential equations are not possible. Ideally, either technique reduces the instrumentation requirements to selection of the state variable that can be measured most accurately.

The application of the quasilinearization techniques is illustrated by identifying the unknown parameters of several one-degree-of-freedom systems. The examples presented apply to the dynamics of a linear and a nonlinear oscillator, a free-falling parachute, and a coasting automobile. Several numerical experiments are presented to relate the effects of noisy boundary conditions to the accuracy with which the coefficients and the initial conditions of the governing differential equations can be computed.

SYMBOLS

A, B, C, D, a	differential-equation coefficients
C	coefficient matrix
$C_D S$	aerodynamic drag-area parameter
$\vec{d}$	inversion vector of the coefficient matrix and α
$E = C^T C$	
$\vec{e} = C^T \vec{d}$	

g	acceleration of gravity, ft/sec^2
J	Jacobian matrix
L	number of boundary conditions
M	vehicle mass, slugs
n	index
P	number of dependent variables in $\vec{Z}$
$\vec{R}(\vec{x})$	residue-equation vector
$R_m(\vec{x})$	residue equation of the form $R_m(x) = R_m\left(x_1, x_2, \ldots, x_m\right) = 0$
S	individual boundary conditions
t	time, sec
x	displacement (height), ft
$x_0, \dot{x}_0, y_0, \dot{y}_0, u, \xi, \lambda$	state variables
y	dependent condition variable
$\vec{Z}$	vector of dependent variables Z
z	state-variable component
α	parameter specified to ensure satisfaction of the boundary conditions
μ	rolling friction coefficient
ρ	air density, slugs/ft^3

Subscripts:

0	initial
i, k, m, n	indices

Superscripts:

(0)	particular solution
(i)	homogeneous solution, i = 1, 2, 3
T	transpose

Operators:

$(\dot{})$	first derivative with respect to time
$(\ddot{})$	second derivative with respect to time

SYSTEM-IDENTIFICATION TECHNIQUES

System identification is the process of fitting the governing differential equations to a given set of boundary conditions. The process involves the determination of the coefficients and initial conditions that satisfy the given set of boundary conditions. The coefficients and initial conditions of the differential equations are referred to as the unknown parameters of the mathematical model.

To illustrate the concept of system identification, the example is considered in which the governing differential equations are

$$\frac{dy}{dt} = ay \tag{1}$$

and

$$\frac{da}{dt} = 0 \tag{2}$$

where a is an unknown parameter. The solution of equation (1) can be determined by straightforward integration. If the range of interest is from zero to t, then the solution to the governing differential equation can be written as

$$y = y_0 e^{at} \tag{3}$$

where y_0 is the initial condition. If the desired solution must satisfy specified boundary conditions such as $y = y_1$ at $t = t_1$ and $y = y_2$ at $t = t_2$, then

$$a = \frac{1}{t_1 - t_2} \ln \frac{y_1}{y_2} \tag{4}$$

and

$$y_0 = y_2 \exp\left(- \frac{t_2}{t_1 - t_2} \ln \frac{y_1}{y_2}\right) \tag{5}$$

Thus, system identification is straightforward for a system that can be described by a differential equation as simple as equation (1). Although equation (1) is linear, the identification problem is nonlinear.

In a more complex differential equation such as

$$\frac{d^2y}{dt^2} + \lambda^2 y = 0 \tag{6}$$

the apparent solution

$$y = A \sin \lambda t + B \cos \lambda t \tag{7}$$

where A and B are arbitrary parameters, is again straightforward. If at $t = 0$, $y = y_0$ and $\dot{y} = \dot{y}_0$, then

$$A = \frac{\dot{y}_0}{\lambda} \tag{8}$$

and

$$B = y_0 \tag{9}$$

Equation (7) can now be written as

$$y = y_0 \cos \lambda t + \frac{\dot{y}_0}{\lambda} \sin \lambda t \tag{10}$$

To determine y_0, $\dot{y}_0$, and λ, the following three independent boundary conditions for y(t) are necessary:

1. $y = y_1$ at $t = t_1$
2. $y = y_2$ at $t = t_2$
3. $y = y_3$ at $t = t_3$

Use of the data points t_1, t_2, and t_3 and equation (10) gives

$$\left.\begin{aligned} y_1 &= y_0 \cos \lambda t_1 + \frac{\dot{y}_0}{\lambda} \sin \lambda t_1 \\ y_2 &= y_0 \cos \lambda t_2 + \frac{\dot{y}_0}{\lambda} \sin \lambda t_2 \\ y_3 &= y_0 \cos \lambda t_3 + \frac{\dot{y}_0}{\lambda} \sin \lambda t_3 \end{aligned}\right\} \tag{11}$$

which are independent equations if the spacing of the data points is properly chosen. The presence of the sine and cosine functions indicates that this set of equations is nonlinear. To determine y_0, $\dot{y}_0$, and λ, an iterative technique (such as the Newton-Raphson method discussed in another section of this report) for solving nonlinear equations is required.

The governing differential equations are always written as a set of first-order equations, and unknown constant parameters are incorporated by adding a null equation.

Thus, equation (6) is written as

$$\left.\begin{aligned} \frac{dy}{dt} &= z \\ \frac{dz}{dt} &= -\xi y \\ \frac{d\xi}{dt} &= 0 \end{aligned}\right\} \tag{12}$$

where

$$\xi = \lambda^2 \tag{13}$$

From the discussion of equations (1) and (6), it is obvious that the problem of system identification is difficult when attempted analytically. With the aid of the digital computer, numerical techniques are available for the solution of complicated system-identification problems. A discussion of quasilinearization techniques and their application to system identification are presented in the following sections of this report.

QUASILINEARIZATION TECHNIQUES

The concept of quasilinearization is presented in the theory of dynamic programming (ref. 1). Quasilinearization techniques provide a systematic, iterative approach for solving linear and nonlinear algebraic and differential equations. Taylor and Ilift (ref. 2) have successfully applied a Newton-Raphson method to the solution of the system-identification problem of determining aerodynamic stability derivatives from flight data. Several other methods are being used in system-identification problems; examples are given in references 3 and 4.

Newton-Raphson Method

The theoretical development of the Newton-Raphson method is based on a Taylor-series expansion of several variables. For example, the vector $\vec{R}(\vec{x})$ represents a set

of residue equations of the form

$$\left.\begin{aligned} R_1(\vec{x}) &= R_1(x_1, x_2, \ldots, x_m) = 0 \\ R_2(\vec{x}) &= R_2(x_1, x_2, \ldots, x_m) = 0 \\ &\vdots \\ R_m(\vec{x}) &= R_m(x_1, x_2, \ldots, x_m) = 0 \end{aligned}\right\} \tag{14}$$

Expanding $\vec{R}(\vec{x})$ in a Taylor series about an approximate solution vector $\vec{x}_n$ obtained in the nth iteration gives

$$\left[\vec{R}(\vec{x})\right]_{n+1} = \left[\vec{R}(\vec{x})\right]_n + \left[\frac{\partial \vec{R}(\vec{x})}{\partial \vec{x}}\right]_n \left(\vec{x}_{n+1} - \vec{x}_n\right) + \ldots \tag{15}$$

If $\vec{x}_{n+1} - \vec{x}_n$ is sufficiently small, the higher order terms of equation (15) can be neglected. Thus

$$\left[\vec{R}(\vec{x})\right]_{n+1} = \left[\vec{R}(\vec{x})\right]_n + \left[\frac{\partial \vec{R}(\vec{x})}{\partial \vec{x}}\right]_n \left(\vec{x}_{n+1} - \vec{x}_n\right) \tag{16}$$

In the final iteration, the residue vector $\vec{R}(\vec{x})$ must become zero for the vector $\vec{x}$ to be a solution; equation (16) is then written as

$$\left[\vec{R}(\vec{x})\right]_n + \left[\frac{\partial \vec{R}(\vec{x})}{\partial \vec{x}}\right]_n \left(\vec{x}_{n+1} - \vec{x}_n\right) = 0 \tag{17}$$

or as

$$\begin{bmatrix} R_1(\vec{x}) \\ R_2(\vec{x}) \\ \vdots \\ R_m(\vec{x}) \end{bmatrix}_n + \begin{bmatrix} \frac{\partial R_1(\vec{x})}{\partial x_1} & \frac{\partial R_1(\vec{x})}{\partial x_2} & \cdots & \frac{\partial R_1(\vec{x})}{\partial x_m} \\ \frac{\partial R_2(\vec{x})}{\partial x_1} & \frac{\partial R_2(\vec{x})}{\partial x_2} & \cdots & \frac{\partial R_2(\vec{x})}{\partial x_m} \\ \vdots & \vdots & & \vdots \\ \frac{\partial R_m(\vec{x})}{\partial x_1} & \frac{\partial R_m(\vec{x})}{\partial x_2} & \cdots & \frac{\partial R_m(\vec{x})}{\partial x_m} \end{bmatrix}_n \begin{bmatrix} x_{1,n+1} - x_{1,n} \\ x_{2,n+1} - x_{2,n} \\ \vdots \\ x_{m,n+1} - x_{m,n} \end{bmatrix} = 0 \qquad (18)$$

in matrix form.

Denoting the Jacobian matrix by J

$$\begin{bmatrix} \frac{\partial R_1(\vec{x})}{\partial x_1} & \frac{\partial R_1(\vec{x})}{\partial x_2} & \cdots & \frac{\partial R_1(\vec{x})}{\partial x_m} \\ \frac{\partial R_2(\vec{x})}{\partial x_1} & \frac{\partial R_2(\vec{x})}{\partial x_2} & \cdots & \frac{\partial R_2(\vec{x})}{\partial x_m} \\ \vdots & \vdots & & \vdots \\ \frac{\partial R_m(\vec{x})}{\partial x_1} & \frac{\partial R_m(\vec{x})}{\partial x_2} & \cdots & \frac{\partial R_m(\vec{x})}{\partial x_m} \end{bmatrix}_{\vec{x}=\vec{x}_n} = J_n \qquad (19)$$

equation (18) is written in vector form as

$$\vec{x}_{n+1} = \vec{x}_n - J_n^{-1}\left[\vec{R}(\vec{x})\right]_n \qquad (20)$$

Equation (20) is the recurrence relation for the Newton-Raphson algorithm, which converges rapidly when the initial guess vector $\vec{x}$ is in the convergence space. Problems arise when irregularities occur in the individual equations. The Newton-Raphson method has, for many problems, the properties of quadratic and monotone convergence (ref. 5).

In an application of the Newton-Raphson algorithm, the nonlinear algebraic equations (eq. (11)) are written as

$$\left.\begin{aligned} R_1(\vec{x}) &= y_0 \cos \lambda t_1 + \frac{\dot{y}_0}{\lambda} \sin \lambda t_1 - y_1 = 0 \\ R_2(\vec{x}) &= y_0 \cos \lambda t_2 + \frac{\dot{y}_0}{\lambda} \sin \lambda t_2 - y_2 = 0 \\ R_3(\vec{x}) &= y_0 \cos \lambda t_3 + \frac{\dot{y}_0}{\lambda} \sin \lambda t_3 - y_3 = 0 \end{aligned}\right\} \tag{21}$$

The Jacobian matrix is

$$\begin{bmatrix} \left[\cos \lambda t_1\right] & \left[\frac{1}{\lambda} \sin \lambda t_1\right] & \left[-\left(y_0 t_1 + \frac{\dot{y}_0}{\lambda^2}\right)\sin \lambda t_1 + \frac{\dot{y}_0 t_1}{\lambda} \cos \lambda t_1\right] \\ \left[\cos \lambda t_2\right] & \left[\frac{1}{\lambda} \sin \lambda t_2\right] & \left[-\left(y_0 t_2 + \frac{\dot{y}_0}{\lambda^2}\right)\sin \lambda t_2 + \frac{\dot{y}_0 t_2}{\lambda} \cos \lambda t_2\right] \\ \left[\cos \lambda t_3\right] & \left[\frac{1}{\lambda} \sin \lambda t_3\right] & \left[-\left(y_0 t_3 + \frac{\dot{y}_0}{\lambda^2}\right)\sin \lambda t_3 + \frac{\dot{y}_0 t_3}{\lambda} \cos \lambda t_3\right] \end{bmatrix} = J \tag{22}$$

Using the recurrence equation (eq. (20)), $\vec{x}$ and $\vec{R}(\vec{x})$ are defined by

$$\vec{x} = \begin{bmatrix} y_0 \\ \dot{y}_0 \\ \lambda \end{bmatrix} \qquad \vec{R}(\vec{x}) = \begin{bmatrix} R_1(\vec{x}) \\ R_2(\vec{x}) \\ R_3(\vec{x}) \end{bmatrix} \tag{23}$$

Two initial guess vectors for $\vec{x}$ are selected to show the convergent properties of the problem. Values of y_0, $\dot{y}_0$, and λ are presented in table I for each iteration of the initial estimate vectors of (0, 1, 1) and (0.5, 0.5, 0.5). The following are boundary conditions to be satisfied:

1. $y_1 = 1.00$ at $t_1 = 0.0$

2. $y_2 = 1.36$ at $t_2 = 0.5$

3. $y_3 = 1.38$ at $t_3 = 1.0$

TABLE I. - NEWTON-RAPHSON ITERATIVE SOLUTION TO EQUATIONS (11)

State variable	Initial guess	Iteration				
		1	2	3	4	5
y_0	0.0000	1.0000	--	--	--	--
$\dot{y}_0$	1.0000	1.0000	--	--	--	--
λ	1.0000	1.0000	--	--	--	--
y_0	0.5000	0.98409	0.741428	1.001728	0.9999	1.0000
$\dot{y}_0$	.5000	1.0000	1.00000	1.00000	1.0000	1.0000
λ	.5000	1.0000	.92949	1.00861	1.0000	1.0000

Newton-Raphson-Kantorovich Method

The Newton-Raphson-Kantorovich method is an extension of the Newton-Raphson method to "function space" (ref. 6). The concept of function space, as explained by Lanczos (ref. 7), involves the replacement of a continuous function by a vector so that the vector describes the continuous function by a set of discrete points.

The Newton-Raphson-Kantorovich method involves the solution of a set of linear differential equations with varying coefficients. In this set of equations, the solution of the linear differential equation converges, under appropriate conditions, to the solution of the nonlinear differential equations. Since the equations are linear and the principle of superposition applies, the boundary conditions can be satisfied at each iteration.

The development of the Newton-Raphson-Kantorovich algorithm starts with the consideration of the first-order vector differential equation

$$\dot{\vec{Z}} = \vec{f}(\vec{Z}, t) \tag{24}$$

where $\vec{Z}$ is composed of P dependent variables, and t is the independent time variable. Expanding equation (24) in function space gives

$$\dot{\vec{Z}}_{n+1} = \left[\vec{f}(\vec{Z}, t)\right]_n + \left[\frac{\partial \vec{f}(\vec{Z}, t)}{\partial \vec{Z}}\right]_n \left(\vec{Z}_{n+1} - \vec{Z}_n\right) + \ldots \tag{25}$$

Neglecting the higher order terms and rewriting gives

$$\dot{\vec{Z}}_{n+1} = \left[\vec{f}(\vec{Z}, t)\right]_n + \left[\frac{\partial \vec{f}(\vec{Z}, t)}{\partial \vec{Z}}\right]_n \vec{Z}_{n+1} - \left[\frac{\partial \vec{f}(\vec{Z}, t)}{\partial \vec{Z}}\right]_n \vec{Z}_n \tag{26}$$

Equation (26) is now written in the form

$$\dot{\vec{Z}}_{n+1} = A_n \vec{Z}_{n+1} + \vec{B}_n \tag{27}$$

where

$$A_n = \left[\frac{\partial \vec{f}(\vec{Z}, t)}{\partial \vec{Z}}\right]_n \qquad \vec{B}_n = \left[\vec{f}(\vec{Z}, t)\right]_n - \left[\frac{\partial \vec{f}(\vec{Z}, t)}{\partial \vec{Z}}\right]_n \vec{Z}_n \tag{28}$$

The vectors $\dot{\vec{Z}}$ and $\vec{Z}$ are linear with respect to the $n + 1$ solution. The A_n and $\vec{B}_n$ terms in equation (27) are known functions that are calculated from the known nth solution or from the previous iteration. In the $n + 1$ solution, the functions A_n and $\vec{B}_n$ reflect the nonlinearity of the original differential equations. By using the recurrence relation (eq. (27)), successive approximations are made to the nonlinear solutions until the desired accuracy is achieved.

Equation (27) is linear with varying coefficients and is easily solved through superposition. The particular solution is a solution of equation (27) with appropriate initial conditions. The vector $\vec{Z}^{(0)}_{n+1}(t)$ denotes this particular solution. The homogeneous solutions are governed by

$$\dot{\vec{Z}}^{(i)}_{n+1}(t) = A_n \vec{Z}^{(i)}_{n+1}(t) \qquad 1 \le i \le P \tag{29}$$

where P is the number of homogeneous solutions. The initial conditions for the homogeneous solutions are selected so that the solutions will be linearly independent. The total solution of equation (27) is

$$\vec{Z}_{n+1}(t) = \vec{Z}^{(0)}_{n+1}(t) + \sum_{i=1}^{P} \alpha_i \vec{Z}^{(i)}_{n+1}(t) \tag{30}$$

where the α_i are specified to ensure satisfaction of the boundary conditions. The particular solution is $\vec{Z}^{(0)}_{n+1}(t)$, and the homogeneous solutions are the $\vec{Z}^{(i)}_{n+1}(t)$.

The initial conditions for the particular and homogeneous solutions should show all the information known about the desired solution. Thus, the initial condition (t = 0) for the particular solution is

$$\vec{Z}^{(0)}_{n+1}(t) = \vec{Z}_n{}^{(0)}(t) + \sum_{i=1}^{P} \alpha_i \vec{Z}_n{}^{(i)}(t) \tag{31}$$

where the right-hand side of equation (31) is known from the previous iteration. The initial conditions for the homogeneous solutions are designated to be approximately the same, except that arbitrary perturbations of elements of these vectors are made to ensure that

$$\det\left(\vec{Z}^{(1)}_{n+1}(t) \;\middle|\; \ldots \;\middle|\; \vec{Z}^{(P)}_{n+1}(t)\right)_{t=0} \neq 0 \tag{32}$$

These strategies ensure that $\alpha_i \to 0$ as convergence is approached and therefore that a straightforward indication of convergence is obtained.

The number of boundary conditions is denoted by L. The individual boundary conditions are denoted by S_k $(1 \leq k \leq L)$. These boundary conditions are placed on elements of $\vec{Z}_{n+1}(t)$ and are satisfied by

$$S_k = \left[\vec{Z}^{(0)}_{n+1}(t_k)\right] + \sum_{i=1}^{P} \alpha_i \left[\vec{Z}^{(i)}_{n+1}(t_k)\right] \qquad 1 \leq k \leq L \tag{33}$$

where t_k is the time at which S_k is measured.

If $L = P$, the following matrix equation yields the α_i upon inversion of the coefficient matrix.

$$C\vec{\alpha} = \vec{d} \tag{34}$$

where

$$C_{ij} = \left[\vec{Z}^{(j)}_{n+1}(t_i)\right] \tag{35}$$

defines the elements of the coefficient matrix. The elements of the right-hand vector are defined by

$$d_i = S_i - \left[\vec{Z}^{(0)}_{n+1}(t_i)\right] \tag{36}$$

If $L > P$ and all boundary conditions are to be satisfied in a least-squares sense, the following matrix equation

$$E\vec{\alpha} = \vec{e} \tag{37}$$

is used, where

$$\left.\begin{aligned} E &= C^T C \\ \vec{e} &= C^T \vec{d} \end{aligned}\right\} \tag{38}$$

When the appropriate matrix-inversion technique is used, the α's are easily determined from equation (37).

Once the vector $\vec{\alpha}$ is determined, the solution and initial conditions for the nonlinear differential equations are updated for the next iteration. The updated solution vector is calculated by using equation (31). The updated initial conditions are also calculated by using equation (31) and letting $t = 0$. The process is repeated with the updated solution and initial conditions until the desired accuracy is achieved.

In an application of the Newton-Raphson-Kantorovich algorithm, the second-order differential equation is written as

$$\ddot{x} + \xi x = 0 \tag{39}$$

where the observed responses or boundary conditions are

1. $x = S_1$ at $t = t_1$
2. $x = S_2$ at $t = t_2$
3. $x = S_3$ at $t = t_3$

The initial conditions x_0, $\dot{x}_0$, and ξ are now determined in order to satisfy the specified boundary conditions. Equation (39) is reduced to two first-order differential equations.

$$\dot{x} = u \tag{40}$$

and

$$\dot{u} = -\xi x \tag{41}$$

Since ξ is a constant

$$\dot{\xi} = 0 \tag{42}$$

Three first-order differential equations are then formed.

$$\left.\begin{aligned} \dot{\vec{Z}} &= \begin{bmatrix} \dot{x} \\ \dot{u} \\ \dot{\xi} \end{bmatrix} \qquad \vec{Z} = \begin{bmatrix} x \\ u \\ \xi \end{bmatrix} \\ & \dot{Z}_1 = Z_2 \\ & \dot{Z}_2 = -Z_1 Z_3 \\ & \dot{Z}_3 = 0 \end{aligned}\right\} \tag{43}$$

Equation (39) is expanded according to equation (27).

$$\dot{x}_{n+1} = u_{n+1} \tag{44}$$

$$\dot{u}_{n+1} = -\xi_n x_n - \xi_n\left(x_{n+1} - x_n\right) - x_n\left(\xi_{n+1} - \xi_n\right) = -\xi_n x_{n+1} - \xi_{n+1} x_n + x_n \xi_n \tag{45}$$

and

$$\dot{\xi}_{n+1} = 0 \tag{46}$$

(Although equation (39) is linear, the same procedure applies if equation (39) is nonlinear. The procedure is independent of whether or not a closed-form solution exists.) Before particular and homogeneous solutions can be determined, an initial guess must be made for the vector $\left[\vec{Z}(t)\right]_{t=0}$.

$$\left[\vec{Z}(t)\right]_{t=0} = \begin{bmatrix} x_0 \\ u_0 \\ \xi \end{bmatrix} \tag{47}$$

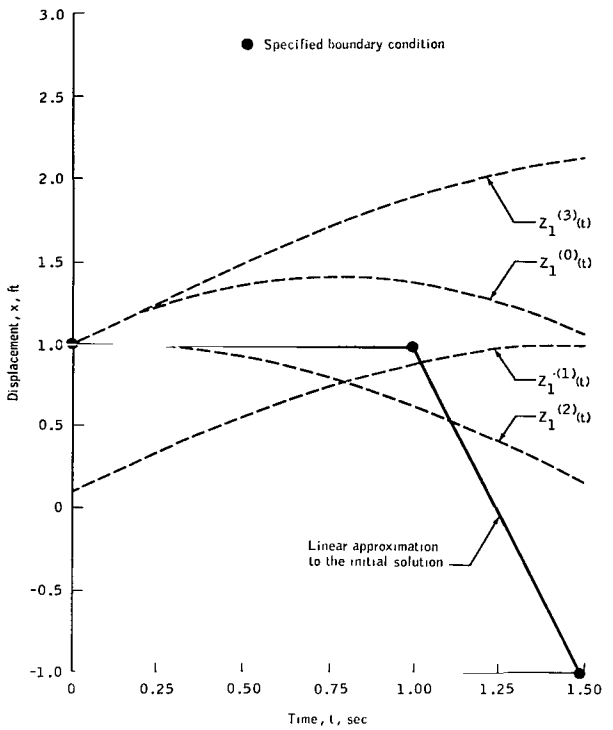

Figure 1. - The first iterative solutions to equations (27) and (29) for the initial conditions defined in equations (48) and (49).

An initial guess must also be made for the solution of the governing differential equation (eq. (39)). A first approximation can be made by using linear interpolation between the specified boundary conditions, as shown in figure 1. The assumed solutions and initial conditions are needed to calculate the n subscripted terms in equation (27).

By using the initial conditions that result in linearly independent solutions, the homogeneous and nonhomogeneous equations are numerically integrated over the time interval of interest such as t_1 to t_3.

The initial conditions for the nonhomogeneous solution (eq. (27)) are

$$\vec{Z}_1^{(0)}(0) = \begin{bmatrix} x_0 \\ u_0 \\ \xi \end{bmatrix} = \begin{bmatrix} 1.00000 \\ 1.00000 \\ 1.00000 \end{bmatrix} \tag{48}$$

The initial conditions for the homogeneous solution (eq. (29)) are

$$\vec{Z}_1^{(1)}(0) = \begin{bmatrix} 0.10000 \\ 1.00000 \\ 1.00000 \end{bmatrix} \quad \vec{Z}_1^{(2)}(0) = \begin{bmatrix} 1.00000 \\ 0.10000 \\ 1.00000 \end{bmatrix} \quad \vec{Z}_1^{(3)}(0) = \begin{bmatrix} 1.00000 \\ 1.00000 \\ 0.10000 \end{bmatrix} \tag{49}$$

From equation (32), it is obvious that these initial conditions result in linear independent solutions. The diagonal elements of the matrix of initial conditions for the homogeneous solutions are perturbed by a factor of 0.10000 for each iteration to ensure linear independence of the solutions. The perturbation factor is a specified parameter that can vary in magnitude depending on the type of problems being solved. The solutions to equations (27) and (29) for the previously discussed initial conditions are shown in figure 1. To ensure fast convergence, the selection of the starting values for the initial conditions should reflect the best available values of the initial conditions. By using equation (33), three linear independent equations are formed.

$$\left.\begin{aligned}
\tilde{S}_1 &= \tilde{Z}^{(0)}_{n+1}(t_1) + \alpha_1 \tilde{Z}^{(1)}_{n+1}(t_1) + \alpha_2 \tilde{Z}^{(2)}_{n+1}(t_1) + \alpha_3 \tilde{Z}^{(3)}_{n+1}(t_1) \\
\tilde{S}_2 &= \tilde{Z}^{(0)}_{n+1}(t_2) + \alpha_1 \tilde{Z}^{(1)}_{n+1}(t_2) + \alpha_2 \tilde{Z}^{(2)}_{n+1}(t_2) + \alpha_3 \tilde{Z}^{(3)}_{n+1}(t_2) \\
\tilde{S}_3 &= \tilde{Z}^{(0)}_{n+1}(t_3) + \alpha_1 \tilde{Z}^{(1)}_{n+1}(t_3) + \alpha_2 \tilde{Z}^{(2)}_{n+1}(t_3) + \alpha_3 \tilde{Z}^{(3)}_{n+1}(t_3)
\end{aligned}\right\} \qquad (50)$$

If the boundary conditions are specified displacements, the vector equation (50) is reduced to a scalar equation. The scalars are the displacement component of the vector $\tilde{Z}$. In this instance, the following specified boundary conditions are displacements:

1. $S_1 = 1.00$ at $t_1 = 0.00$
2. $S_2 = 1.00$ at $t_2 = 1.00$
3. $S_3 = -1.00$ at $t_3 = 1.50$

When the displacement component of the vector $\tilde{Z}$ is used as specified in figure 1, the three linear independent equations (eq. (50)) are reduced to

$$\left.\begin{aligned}
1.00 &= 1.00 + 0.10\alpha_1 + 1.00\alpha_2 + 1.00\alpha_3 \\
1.00 &= 1.38 + 0.89\alpha_1 + 0.62\alpha_2 + 1.89\alpha_3 \\
-1.00 &= 1.04 + 1.01\alpha_1 + 0.17\alpha_2 + 2.14\alpha_3
\end{aligned}\right\} \qquad (51)$$

Once the homogeneous and nonhomogeneous solutions have been determined, a standard matrix-inversion technique is used to determine the unknown α's. After the α's have been determined, the solution to the governing differential equation is updated by using equation (31). The initial conditions and coefficients are also updated by using equation (31). The process is repeated with the updated solution and initial conditions until convergence has been achieved. Values for x_0, $\dot{x}_0$, and ξ are presented in table II for each iteration on the solution to illustrate the convergent characteristics of this algorithm.

TABLE II. - NEWTON-RAPHSON-KANTOROVICH ITERATIVE

SOLUTION TO EQUATION (39)

State variable	Exact solution	Initial guess	Iteration					
			1	2	3	4	5	6
x_o	1.00000	1.00000	1.00000	1.00000	1.00000	1.00000	1.00000	1.00000
$\dot{x}_o$	1.20924	1.00000	.684269	1.03947	1.19223	1.20907	1.20924	1.20924
ξ	4.38681	1.00000	2.46593	3.85735	4.33703	4.38633	4.38681	4.38681

APPLICATIONS

The quasilinearization techniques for solving system-identification problems can be applied to many categories of dynamics and related fields. The examples discussed in this report are confined to problems involving the dynamics of several one-degree-of-freedom systems. The numerical examples are designed to relate the accuracy of the observations of the pertinent state variable to the accuracy to which the coefficients and initial conditions of the governing differential equation are calculated. Specific applications of a quasilinearization technique to the system-identification problems of parachute dynamics and automobile coasting dynamics are discussed.

Numerical Examples

The following nonlinear ordinary second-order differential equation is used for one set of numerical examples to relate the effect of noisy boundary conditions on the determination of the coefficients and initial conditions.

$$\frac{d^2y}{dt^2} + A\frac{dy}{dt} + By + C\left(\frac{dy}{dt}\right)^3 + Dy^3 = 0 \tag{52}$$

The independent variable t is time, and the dependent variable y is displacement. The initial conditions on y and dy/dt and the coefficients A, B, C, and D are selected so that oscillatory motion results.

If the coefficients C and D are set equal to zero, equation (52) reduces to the linear ordinary second-order differential equation

$$\frac{d^2y}{dt^2} + A\frac{dy}{dt} + By = 0 \tag{53}$$

which will be used as the governing differential equation for the second set of numerical examples.

Equation (52) is analogous to a spring-mass system with linear and nonlinear properties of spring and damping forces. To develop precision data for the displacement history for equations (52) and (53), values for the coefficients and initial conditions were assigned and numerically integrated (ref. 8). The displacement data developed by numerical integration have six-digit accuracy. Noise was superimposed on the integrated displacement data by rounding off the six-digit-accurate displacement values to four- and two-digit accuracy. By making the numerically integrated data analogous to experimentally measured data, the Newton-Raphson-Kantorovich method is applied to the problem of identifying the differential-equation coefficients and initial conditions which best fit the experimental data. The degrees of accuracy of the numerically integrated data are assumed to be analogous to experimental error.

Comparisons are presented in table III for the initial conditions and coefficients computed by using quasilinearization for the nonlinear differential equation (eq. (52)).

TABLE III. - TABULATED VALUES OF INITIAL CONDITIONS AND COEFFICIENTS FOR EQUATION (52)[a]

State variable or coefficient	Exact solution	6-digit accuracy	4-digit accuracy	2-digit accuracy
y_0	0.00000	-0.000001	0.000010	-0.001527
$\dot{y}_0$	1.00000	1.00002	.999846	1.02469
A	.10000	.100027	.100171	.059754
B	3.00000	3.00015	2.99986	2.99733
C	.20000	.199912	.199583	.303364
D	4.00000	4.00063	4.00348	4.03972

[a]Fourteen specified displacements obtained every 0.5 second from $t = 0$ to $t = 6.5$.

In this computation, six-, four-, and two-digit accuracy was used on the specified displacement history. The specified displacements were obtained at intervals of 0.5 second from $t = 0$ to $t = 6.5$ seconds. For example, if the boundary conditions in in table III are specified to four-digit accuracy, the coefficient A is calculated to be 0.100171, as compared to the exact value of 0.100000 for A. Similar comparisons for the linear differential equation (eq. (53)) are presented in table IV.

TABLE IV. - TABULATED VALUES OF INITIAL CONDITIONS AND COEFFICIENTS FOR EQUATION (53)[a]

State variable or coefficient	Exact solution	6-digit accuracy	4-digit accuracy	2-digit accuracy
y_0	0.0000	0.000000	0.000000	-0.001870
$\dot{y}_0$	1.00000	1.00002	1.00001	1.00012
A	.100000	.099999	.100030	.102050
B	3.00000	3.00015	3.00015	3.00104

[a]Fourteen specified displacements obtained every 0.5 second from $t = 0$ to $t = 6.5$.

The data in tables III and IV indicate that the initial conditions are calculated to the same accuracy as the specified data for the examples studied. The coefficients, however, have the same accuracy as the specified data for the linear differential equation (eq. (53)) and one less digit of accuracy for the nonlinear differential equation (eq. (52)). This difference in accuracy is probably attributed to the higher ratio of the specified displacement data to the differential-equation parameters (initial conditions and coefficients). The time span for which the displacement data are specified also influences computed parameter accuracy.

Parachute Dynamics

The Newton-Raphson-Kantorovich method of solving system-identification problems is also applied to parachute dynamics. Parachutes are used primarily as aerodynamic deceleration devices. The normal sequence of parachute deployment is ejection from the payload, inflation or opening (which may be controlled or uncontrolled), and subsequent descent.

The parachute dynamics during inflation are difficult to model mathematically because of changing parachute geometry, virtual mass effects, et cetera. The descent

dynamics after the parachute has stabilized from the inflation process are more straightforward. The dynamics of the parachute trajectory are approximated with good accuracy by the second-order nonlinear differential equation

$$\frac{d^2x}{dt^2} + C_D S \frac{\rho}{2M}\left(\frac{dx}{dt}\right)^2 = g \tag{54}$$

where x is displacement (height) in feet, t is time in seconds, M is payload mass in slugs, $C_D S$ is a drag-area parameter in square feet, ρ is air density in slugs per cubic feet, g is acceleration of gravity in feet per second per second, d^2x/dt^2 is vehicle acceleration in feet per second per second, and dx/dt is vehicle velocity in feet per second.

Experimentally measured values of position versus time for a free-falling, fully inflated parachute are presented in table V (ref. 9). These data are for the time span following the parachute inflation process. During this period, the parachute payload system decelerates from the opening velocity to the steady-state velocity, which occurs when aerodynamic drag is equal to parachute payload weight. The fall distance for which the parachute data are taken is approximately 1000 feet. Because of the small change in atmospheric density during this period, the density is assumed constant.

With equation (54) as the governing differential equation, the coefficient and initial conditions are determined by using quasilinearization so that the solution to the differential equation satisfies the experimental displacement data in a least-squares sense (minimizes the square of the deviation). The predicted values of parachute displacement, velocity, acceleration, and drag-area parameter $C_D S$ are presented in table V. The values selected for the drag-area parameter and initial conditions correlate generally within 1 foot of the measured trajectory for a free-fall distance of approximately 1000 feet.

Several numerical experiments are presented that relate the accuracy of the calculated coefficient and the initial conditions of the differential equation to the accuracy of the specified boundary conditions (experimental data). The following differential equations and initial conditions are assumed and numerically integrated to develop precise data for the boundary conditions.

$$\frac{d^2x}{dt^2} + 0.24708 \times 10^{-3}\left(\frac{dx}{dt}\right)^2 = 32.17 \tag{55}$$

$$\left(\frac{dx}{dt}\right)_{t=0} = 443.2 \text{ ft/sec} \tag{56}$$

$$x_{t=0} = 0.0 \tag{57}$$

Values of displacement and velocity are presented in table VI for the solution of equation (55). The tabulated values have six-digit accuracy.

TABLE V.- PARACHUTE DATA[a]

$$\left[C_D S = 147.78 \text{ ft}^2, \quad \rho = 0.1354 \times 10^{-2} \text{ slug/ft}^3, \quad M = 405 \text{ slugs}\right]$$

Time, sec	Experimental displacement, ft	Predicted displacement, ft	Predicted velocity, ft/sec	Predicted acceleration, ft/sec^2
0.0	0.0	0.0	443.20	-16.35
.2	87.5	88.3	440.00	-15.66
.4	176.0	176.0	436.94	-14.99
.6	263.0	263.1	434.00	-14.36
.8	349.2	349.6	431.19	-13.76
1.0	434.7	435.6	428.50	-13.19
1.2	520.8	521.0	425.91	-12.64
1.4	606.7	606.0	423.43	-12.12
1.6	691.7	690.4	421.06	-11.62
1.8	775.0	774.4	418.78	-11.15
2.0	857.6	857.9	416.60	-10.70
2.2	940.2	941.0	414.50	-10.27

[a]These data are a portion of an overall parachute payload trajectory in which several parachutes were deployed at different time sequences. These data were selected because the parachute payload dynamics can be approximated by equation (54).

TABLE VI. - SOLUTION TO EQUATION (55)

Time, sec	Displacement, ft	Velocity, ft/sec
0.0	0.000	443.200
.2	88.317	439.998
.4	176.008	436.932
.6	263.099	433.996
.8	349.615	431.183
1.0	435.580	428.487
1.2	521.017	425.903
1.4	605.948	423.426
1.6	690.394	421.050
1.8	774.375	418.771
2.0	857.909	416.584
2.2	941.014	414.486

The numerically developed data in table VI were rounded off to simulate the experimental error. The results of using data of ±0.001-, ±0.1-, and ±5-foot displacement or position accuracy to determine the accuracy of coefficients and initial conditions are presented in table VII.

The data indicate, for the velocity and time span studied, that the coefficient of the velocity-squared expression and initial velocity can be calculated to within 1 percent for 5-foot position errors. By extrapolating this value to the parachute experimental data, the drag-area parameter C_DS can be calculated to within 1 percent if the experimental position error is within 5 feet.

TABLE VII. - EFFECT OF NOISY BOUNDARY CONDITIONS ON VALUES OF DIFFERENTIAL-EQUATION PARAMETERS

$$\left[\frac{d^2x}{dt^2} + C_1\left(\frac{dx}{dt}\right)^2 = 32.17\right]$$

Parameter	Exact value	Specified boundary-condition accuracy, ft		
		±0.001	±0.1	±5.0
$\left(\frac{dx}{dt}\right)_{t=0}$	443.200	443.200	442.830	443.175
C_1	0.2470800×10^{-3}	0.2470818×10^{-3}	0.2453796×10^{-3}	0.2466957×10^{-3}

Coasting-Automobile Dynamics

The dynamics of a coasting automobile are primarily influenced by two externally applied forces: aerodynamic drag and rolling friction. The aerodynamic drag is considered to be a function of the square of the relative velocity of the automobile (relative to the wind). Rolling friction forces are assumed to be a function of the automobile weight.

The governing differential equation for a coasting automobile for a no-wind condition is

$$\frac{d^2x}{dt^2} + \frac{\rho C_D S}{2M}\left(\frac{dx}{dt}\right)^2 + \mu g = 0 \tag{58}$$

where μ is the rolling friction coefficient.

The differential equation for the coasting dynamics of an automobile is similar to the differential equation for a free-falling parachute. If $\mu = -1$, equation (58) is identical to equation (54). The system-identification problem of the automobile includes the determination of rolling friction coefficient μ.

The experimental data for the coasting automobile are in the form of a velocity-time history (ref. 10). Table VIII presents experimentally measured values of velocity versus time for a coasting automobile. By using equation (58) as the governing differential equation, the coefficients and initial conditions are determined such that a "best" fit on the experimental data was obtained. Also presented in table VIII are the values of velocity, displacement, drag-area parameter $C_D S$, and rolling friction coefficient μ predicted by quasilinearization. To relate the accuracy of the predicted coefficients and initial conditions to the accuracy of the specified boundary conditions,

the differential equation and initial conditions

$$\frac{d^2x}{dt^2} + 1.303065 \times 10^{-4}\left(\frac{dx}{dt}\right)^2 + 0.6671862 = 0 \tag{59}$$

$$x_{t=0} = 0.0 \text{ ft} \tag{60}$$

$$\left(\frac{dx}{dt}\right)_{t=0} = 116.90158 \text{ ft/sec} \tag{61}$$

are numerically integrated. The integrated values of displacement and velocity are considered to be analogous with experimental data of six-digit accuracy.

TABLE VIII. - COASTING-AUTOMOBILE DATA

$$\left[x_{t=0} = 0, \quad (dx/dt)_{t=0} = 116.90158 \text{ ft/sec}, \quad C_D S = 8.80719 \text{ ft}^2, \right.$$
$$\left. \rho = 0.00238 \text{ slug/ft}^3, \quad \mu = 0.0207201, \quad M = 80.43 \text{ slugs} \right]$$

Time, sec	Experimental measured velocity, ft/sec	Predicted velocity, ft/sec (a)	Predicted displacement, ft (a)
0	117.3	116.902	0.000
5	104.9	105.520	555.369
10	95.3	95.604	1057.641
15	87.3	86.852	1513.350
20	79.2	79.038	1927.725
25	71.9	71.990	2305.007
30	65.7	65.574	2648.678
35	59.8	59.684	2961.622
40	54.0	54.235	3246.250

[a]These numerically integrated values have six-digit accuracy.

Numerical experiments were conducted to determine the influence of experimental error on the predicted differential-equation coefficient and initial conditions. Two types of numerical experiments were conducted: in one type of experiment, the velocity data were used as the specified boundary condition, and in the other type of experiment, the displacement data were used as the specified boundary conditions. These experiments were designed to compare the accuracy in computing differential-equation coefficients and initial conditions for specified boundary conditions of different orders. The experimental error was developed by rounding off the integrated data to accuracies of 1 and 5 ft/sec for velocity and to accuracies of 1, 5, and 10 feet for displacement.

Values of initial conditions and coefficients are presented in table IX for each set of data at a given experimental error. For a ±5-foot displacement error, the coefficient C is computed to be 1.30469×10^{-4}, which is within 0.12 percent of the exact value of C_1.

An error of ±10 feet in experimental displacement data results in approximately the same accuracy in computation of the differential-equation parameters as a ±5-ft/sec error in the experimental velocity data. An error of ±5 feet in the displacement data gives better accuracy in the computed differential-equation parameters than a ±1-ft/sec error in the velocity data.

TABLE IX. - EFFECTS OF NOISY BOUNDARY CONDITIONS ON CALCULATED PARAMETERS OF DIFFERENTIAL EQUATION (58)

$$\left[\frac{d^2x}{dt^2} + C_1\left(\frac{dx}{dt}\right)^2 + C_2 = 0, \quad \rho = 0.00238 \text{ slug/ft}^3, \quad C_D S = 2C_1 M/\rho, \quad M = 80.43 \text{ slugs}, \quad \mu = C_2/g\right]$$

Parameter	Exact value	Specified boundary-condition accuracy									
		Displacement						Velocity			
		±1 ft	Percent error (a)	±5 ft	Percent error (a)	±10 ft	Percent error (a)	±1 ft/sec	Percent error (a)	±5 ft/sec	Percent error (a)
$(dx/dt)_{t=0}$, ft/sec	116.902	116.840	0.053	117.147	0.21	117.402	0.42	117.124	0.19	115.534	1.18
C_1	1.30307×10^{-4}	1.28490×10^{-4}	1.41	1.30469×10^{-4}	0.12	1.39411×10^{-4}	6.53	1.27184×10^{-4}	2.45	1.34169×10^{-4}	5.69
C_2	0.667186	0.679847	1.86	0.678837	1.72	0.608339	9.67	0.690197	3.33	0.586287	13.80
$C_D S$, ft^2	0.509086	0.50199	1.41	0.509723	0.12	0.544657	6.53	0.496900	2.45	0.539806	5.69
μ	2.07201×10^{-2}	2.11133×10^{-2}	1.86	2.10819×10^{-2}	1.72	1.88925×10^{-2}	9.67	2.14347×10^{-2}	3.33	1.82077×10^{-2}	13.80

[a] Percent error = $\left|1 - \frac{\text{exact value}}{\text{computed value}}\right| \times 10^{-2}$

CONCLUDING REMARKS

The quasilinearization techniques provide a systematic iterative approach to fitting a governing differential equation (or equations) to a set of measured observations. The advantage of this technique in system identification is that it permits the selection of the state variables that describe the measured observation whether the observation is displacement, velocity, or any other variable. The measured observations can be made from the standpoint of economy, accuracy, or convenience. In terms of economy, this technique may reduce instrumentation requirements.

The accuracy of the predicted differential-equation coefficients and initial conditions is a function of experimental error in the measured observations. Because of the nature of measuring devices, the higher the order of the state variable (such as velocity and acceleration) being measured, the noisier the experimental data. The quasilinearization technique allows the selection of the state variable with the least noise or the lowest order, which is displacement in dynamics problems.

The quasilinearization techniques are applied to the identification of several one-degree-of-freedom systems. Linear and nonlinear systems are used to relate the accuracy of the differential-equation coefficients and initial conditions for a given experimental error in boundary conditions. The data indicate that the initial conditions can be calculated to the same accuracy as the specified boundary conditions (e.g., two-digit-accurate boundary conditions for two-digit-accurate initial conditions), whereas the computed coefficients have less accuracy than the specified boundary conditions.

Specific system-identification problems of the free-falling parachute are discussed. Results indicate, for the conditions studied, that the parachute aerodynamic drag-area parameter can be calculated with good accuracy during a transient, free-falling condition. The numerical examples indicate that the aerodynamic drag-area parameter can be calculated to ±1 percent when errors in parachute position data are as large as 5 feet for the parachute trajectory studied.

Experimental data on the coasting automobile are presented in the form of a velocity history. The system-identification problem for a coasting automobile includes determination of the initial conditions, aerodynamic drag-area parameter, and rolling friction coefficient. Numerical experiments were conducted to relate errors in experimental velocity histories and displacement histories to the predicted accuracy of the differential-equation parameters. The results indicate that determination of the differential-equation parameters is almost twice as accurate when displacement data rather than velocity data with the same order of accuracy are used.

National Aeronautics and Space Administration
Manned Spacecraft Center
Houston, Texas, April 25, 1969
914-13-20-17-72

REFERENCES

1. Bellman, R. E.: Dynamic Programming. Princeton University Press (New Jersey), 1957.

2. Taylor, L. W., Jr.; and Ilift, K. W.: A Modified Newton-Raphson Method for Determining Stability Derivatives from Flight Data. Procedures of the 2nd Annual Conference on Computing Methods in Optimization Problems, Sanremo, Italy, Sept. 1968.

3. Larson, Duane B.; and Fleck, John T.: Identification of Parameters by the Method of Quasilinearization. Cornell Aeronautical Lab, Inc. (Buffalo, N.Y.), Report No. 164, May 1968.

4. Cuenod, M.; and Sage, A. P.: Comparison of Some Methods Used for Process Identification. Automatica, vol. 4, no. 4, May 1968, pp. 235-269.

5. Kalaba, Robert: On Nonlinear Differential Equations, The Maximum Operation, and Monotone Convergence. J. Math. Mech., vol. 8, no. 4, 1959, pp. 519-574.

6. Bellman, R. E.; and Kalaba, R. E.: Quasilinearization and Nonlinear Boundary-Value Problems. American Elsevier Publishing Company, Inc. (New York), 1965.

7. Lanczos, C.: Linear Differential Operators. D. Van Nostrand Company, Ltd. (London), 1961.

8. Doiron, H. H.: Numerical Integration Via Power Series Expansions. M.S. Thesis, University of Houston, 1967.

9. Kelly, E. L.: Project 9103. Philco-Ford Test Drop Report 2508F(67), Jan. 4, 1968.

10. Anon.: Road and Track Road Test Annual for 1966. Bond Publishing Company (Newport Beach, California), 1966.

NASA-Langley, 1969 —— 19 S-211

NATIONAL AERONAUTICS AND SPACE ADMINISTRATION
WASHINGTON, D.C. 20546

OFFICIAL BUSINESS

FIRST CLASS MAIL

POSTAGE AND FEES PAID
NATIONAL AERONAUTICS AND
SPACE ADMINISTRATION

POSTMASTER: If Undeliverable (Section 158 Postal Manual) Do Not Return

"The aeronautical and space activities of the United States shall be conducted so as to contribute . . . to the expansion of human knowledge of phenomena in the atmosphere and space. The Administration shall provide for the widest practicable and appropriate dissemination of information concerning its activities and the results thereof."

—NATIONAL AERONAUTICS AND SPACE ACT OF 1958

NASA SCIENTIFIC AND TECHNICAL PUBLICATIONS

TECHNICAL REPORTS: Scientific and technical information considered important, complete, and a lasting contribution to existing knowledge.

TECHNICAL NOTES: Information less broad in scope but nevertheless of importance as a contribution to existing knowledge.

TECHNICAL MEMORANDUMS: Information receiving limited distribution because of preliminary data, security classification, or other reasons.

CONTRACTOR REPORTS: Scientific and technical information generated under a NASA contract or grant and considered an important contribution to existing knowledge.

TECHNICAL TRANSLATIONS: Information published in a foreign language considered to merit NASA distribution in English.

SPECIAL PUBLICATIONS: Information derived from or of value to NASA activities. Publications include conference proceedings, monographs, data compilations, handbooks, sourcebooks, and special bibliographies.

TECHNOLOGY UTILIZATION PUBLICATIONS: Information on technology used by NASA that may be of particular interest in commercial and other non-aerospace applications. Publications include Tech Briefs, Technology Utilization Reports and Notes, and Technology Surveys.

Details on the availability of these publications may be obtained from:

SCIENTIFIC AND TECHNICAL INFORMATION DIVISION

NATIONAL AERONAUTICS AND SPACE ADMINISTRATION

Washington, D.C. 20546